Strike Slip Faults on Jupiter's Moon Europa

by: Jeffrey Adams

Advisor: Vedran Lekic

GEOL394

November 21, 2017

Abstract:

The surface of Jupiter's moon Europa is covered with numerous overlapping lineaments and markings, many of which represent cracks in the icy crust covering the subsurface ocean. The forces forming and changing these surface lineaments are of tidal origin, which is unusual, when compared with processes operating here on Earth. Some of these lineaments have been interpreted as strike slip faults, because they visibly offset a continuous feature on either side. Existing models strike-slip formation on Europa suggest that offsets across them will be greater when aligned with tidal forces. In this study I test the hypothesis that the azimuth of strike slip faults on Europa will correlate with the accumulated slip of the strike slip faults.

These faults were mapped in ArcGIS, and the geodesic length and azimuth of these offsets collected. A total of 72 strike slip faults were identified, in four regions across the surface of Europa, in which the imagery provided sufficiently high resolution. The azimuth and geodesic length were calculated to have a circular correlation coefficient of 0.162, with an associated p value of 0.388. While positive, this coefficient is therefore not statistically significant enough to reject the null hypothesis for which we would need to observe a p value equal to or less than 0.05. Therefore, we reject the hypothesis, and settle on the null hypothesis that there is not a correlation between bearing and geodesic length. A plausible explanation is that tidal forces are not strong enough to cause these strike slip faults to offset features further in a certain direction than other directions. It could also be hypothesized that the age of the lineaments along offset features has an impact on the correlation of offset and azimuth.

However, fault mapping carried out in this study revealed that in the areas mapped, right lateral faults are more prevalent than those with a left lateral sense. There were 28 left lateral faults found, and 44 right lateral faults which were recorded. Using a binomial probability calculation, there is only a 1.59% chance that such a distribution could be observed at random if left and right lateral faults were equally likely. This statistically significant value would suggest that there are factors influencing the prevalence of one of these attitudes over the other, and is consistent with models of tidal stresses.

In all regions of the map which were studied, there existed unusual features which resemble strike slip faults, but fail to meet all the criteria necessary to be classified as such. These features, termed 'jogs' have not been the focus of any previous study or analysis. Each jog is contained in a single lineament, described by the lineament making sudden changes in direction, often 90°. If the surrounding regions showed any evidence of offset, these would be classified as strike slip faults as well, but the regions on either side of the jogs have no noticeable offset. The average azimuth of these jogs appear to be close to 90° from the average azimuth of strike slip faults in the respective map regions. Further research and a separate study should be performed on these jogs to gain an understanding of plausible causes.

Table Of Contents:

I.	Title Page	1
II.	Abstract	2
III.	Table of Contents	3
IV.	Introduction	4
	Figure 1	
	Figure 2	
	Figure 3	
v.	Method of Analysis	7
	Figure 4	
	Figure 5	
VI.	Presentation of Data	10
	Figure 6	
	Figure 7	
	Figure 8	
VII.	Discussion of Results	12
	Figure 9	
	Figure 10	
VIII	1. Suggestions for Future Work	13
	Figure 11	
	Figure 12	
IX.	Conclusions	15
X.	Bibliography	16
XI.	Appendices	17

Introduction / Background:

Jupiter is the fifth planet from the sun, and the most massive and largest of all of the planets. It has 67 known moons, ranging in sizes comparable to asteroids to objects larger than Earth's Moon. The largest four were observed by Galileo in 1610, which earned them the classification of "Galilean moons." Europa, the main subject of this study, does not have enough gas above the surface to qualify as an atmosphere, so that surface erosion should be less than on surfaces with atmospheres. Yet, instead of being old and pristinely preserved, paradoxically, current estimates place the surface age of Europa at between 30 and 100 Myr (Ip et al., 2000). This estimate is based on the known average impact rate in the Jovian system, of which the only data is available from the Voyager and Galileo missions.

Europa presents evidence of a liquid ocean and an overlying ice shell (Schenk, McKinnon 1985). Schenk and McKinnon suggest that the ice shell is mobile, and presents a Europan tectonic model, with many differences when compared to Earth-like tectonics. The key aspect of Europa's internal structure is the presence of an ocean between the crust and the true silicate mantle (Jin and Ji, 2012). This liquid layer changes the dynamic properties of the icy crust when it is compared to a more traditional 3 layer 'Earth type' mantle and crust system. Jin's model theorizes that the mantle composition beneath this liquid ocean is similar to Earth's, made up of silicates. The core composition in this model, however, differs, and it is posited that the core is made up of FeS, as opposed to the Ni-Fe of Earth. Figure 1 shows the proportions of these layers, which depend on their actual makeup, with the actual ice crust being included as part of "water" (Jin and Ji, 2012).

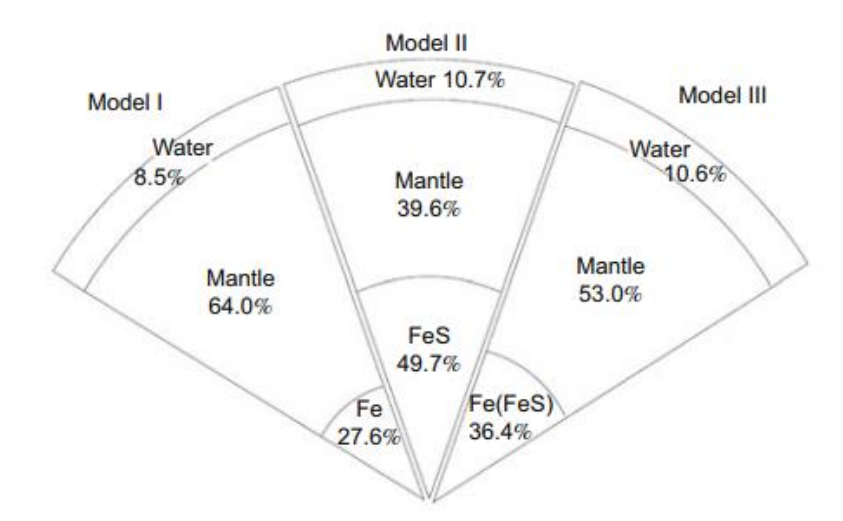


Fig. 1

Three different models of Europa's internal structure showing percentages of each layer by volume. The total radius shown is between 1562 km (model I) and 1569 km (model III).

Model and image constructed by Jin and Ji (2012).

Europa is strongly affected by tidal forces. The majority of the force exerted on Europa's surface is due to Jupiter's gravitational pull. These tidal forces deform the moon, allowing cracks to propagate throughout the surface crust. Carr et al. (1998) hypothesized that the surface lineaments were related to tidal forces, and proposed their abundance as evidence for the existence of a subsurface ocean. Called "Linae" or "Lineaments," these dark surface cracks cover the surface, recording and preserving the different planetary forces that acted upon the icy crust in order to fracture it. The obliquity, or axial tilt, is the angle of difference between the rotational and orbital axes, and is predicted to create different patterns of extensional and compressional stresses on the northern and southern hemispheres. Given the existence of the

subsurface ocean, it was hypothesized that the ice shell may not rotate at the same speed as the rest of the moon, since the ice crust is separated from the silicate mantle underneath (Hoppa, 1972). The term applied to this phenomenon was "non-synchronous rotation," with the crust rotating at a different speed than the mantle. Once theorized to be the cause of the variety of crack types and azimuths present, this hypothesis has since fallen out of favor (Goldreich and Mitchell, 2010). Further research compared ice shell stresses that would result from a non-synchronous model to those due to precession-influenced tides (Rhoden et al., 2012). The precession of this orbital body is the slow rotation of the rotational axis around the orbital axis due to the torque exerted by Jupiter.

Tidal flexing of the ice shell leaves behind cracks and lineaments in the ice shell, with few similarities to faults present on Earth. However, relative contributions of various components of tidal stress that produced many of these faults is still being investigated. One of the important components was hypothesized to have been the obliquity of Europa (Rhoden and Hurford, 2013). This would lead to hemispheres having different tidal forces acting upon them. Many of the surface lineaments have a distinctive cycloid arch shape. These cycloidal fractures go through all geographic regions, and are hypothesized to be the result of tidal stresses due to libration. Libration is the oscillation of the nearest point on the moon with respect to Jupiter, due to the fact that a constant rotation of Europa is faster than the revolution when the moon is further from Jupiter and then slower than the revolution when the moon is closer to Jupiter. As a result, the nearest point of this moon to Jupiter will have a slight change in position, causing periodic changes in the tidal deformation and producing cracks not expected for tides due to ellipticity and obliquity.

It is currently hypothesized that precession has the greatest bearing upon the orientation of surface fractures due to the gravitational forces from the bodies surrounding Europa. Jupiter itself exerts a gravitational pull proportionate to its mass, which easily deforms the ice crust. This effect, coupled with the obliquity of the moon, causes the orientation and right or left-laterality of lineaments on different hemispheres to be correlated (Hoppa et al., 2000). Hoppa noticed that on the northern hemisphere, there is an abundance of left-lateral faults. This observation was linked to the rotation and obliquity of the moon, and led to the theory of 'tidal walking,' where the cracks would slowly move depending on where the gravitational force is present, during the orbital cycle. An image of the predictive model used by Hoppa to predict the proportion of left or right lateral faults at differing latitudes and longitudes is shown in figure 2. This model shows the higher probability for left lateral attitudes in the far north, as well as the increased likelihood for right lateral faults in the far south hemisphere.

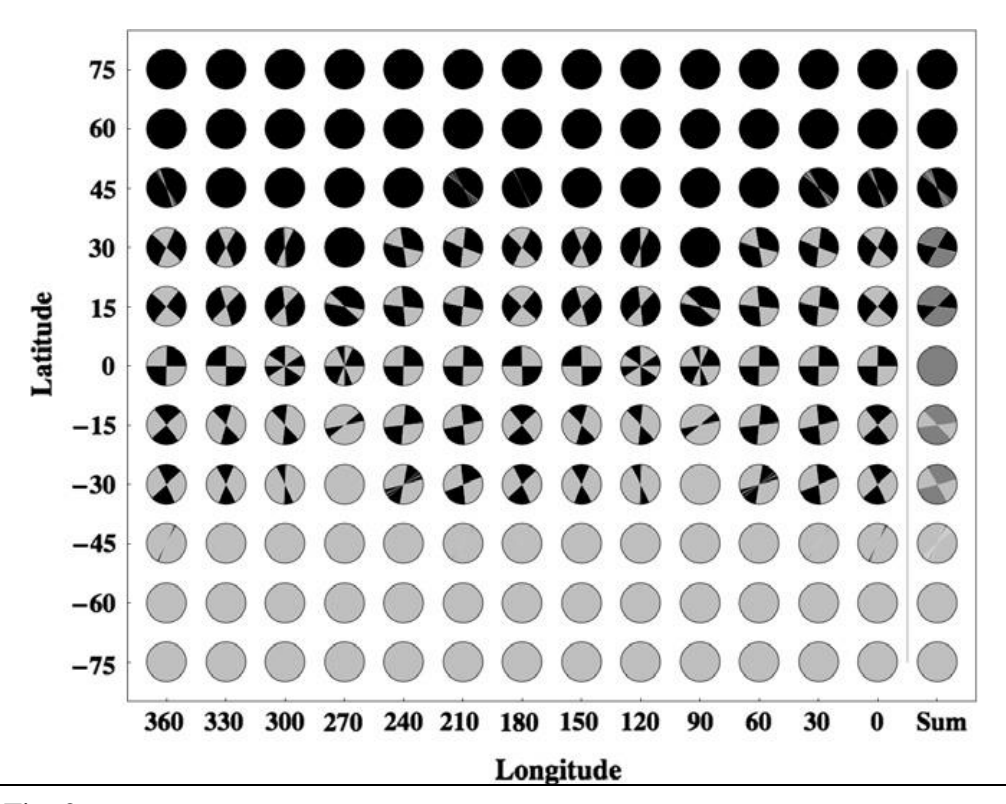


Fig. 2.

Shell tectonics predictions of slip direction with zero obliquity. Within each circle, black regions indicate crack azimuths along which left lateral displacement is predicted; light gray represents right lateral fault azimuths. The last column shows the predictions summed over all longitudes, in which dark gray represents azimuths that could have either attitude of displacement depending on their longitude when displacement occurred.

Image and model generated by Hoppa (2000).

Many of the surface lineaments are not distinct lines, but have ridges or bands that form with varying thicknesses. These features further support the hypothesis of a watery sub layer underneath the crust (Culha et al., 2013). Formed by the contraction and expansion of the crust perpendicular to the ridge direction, the dark bands are raised by the accumulation of material along the initial lineaments. This 'banding' is the site of many slip zones, and can accumulate widths in excess of several kilometers, as shown in figure 3.

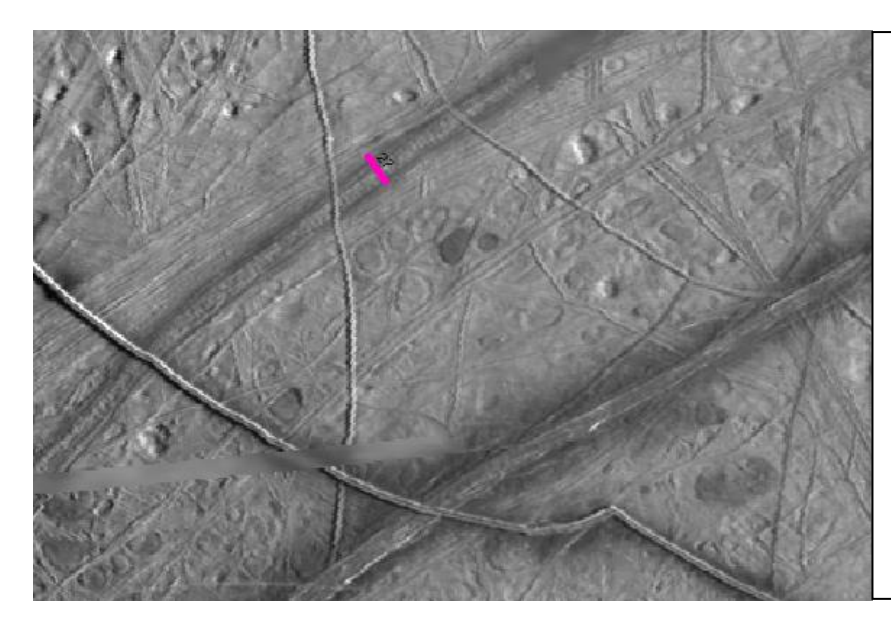


Fig. 3

A double banded ridge is shown, with other lineaments crossing through. The relationship between newer and older faults is shown by the over- and under-laying faults.

The pink line illustrates the width, being 9 km wide.

Method of Analysis:

The information available for analysis here are images taken by the Galileo and Voyager probes aggregated into a global mosaic map. These images cover a majority of the moon's surface, with varying degrees of resolution, as illustrated in figure 4. This aggregated image was loaded into ArcGIS and had a coordinate system applied to it to form a map. There are regions that have been chosen for study, because their spatial resolutions are high enough to perform a proper analysis, and these regions are concentrated in two distinct bands oriented north-south.

In the areas of study, the first step was to visually find lineaments, then identify offset features needed to determine whether they are strike slip faults. I use the ArcGIS software to trace and map them by entering a two point polyline into the coordinate system. This method of tracing the faults generated data that allowed for measuring the azimuth, geodesic length, slip sense (right vs. left lateral), and location. A standard Europan coordinate system is in use (called GCS Europa), and it follows the same principle of latitude and longitude which are in use for the modern Earth based coordinate systems. Another easting and northing coordinate system was also in place, called the Cylindrical Europa model, although this coordinate system was mainly used for background calculation and measurement by the ArcGIS program itself.

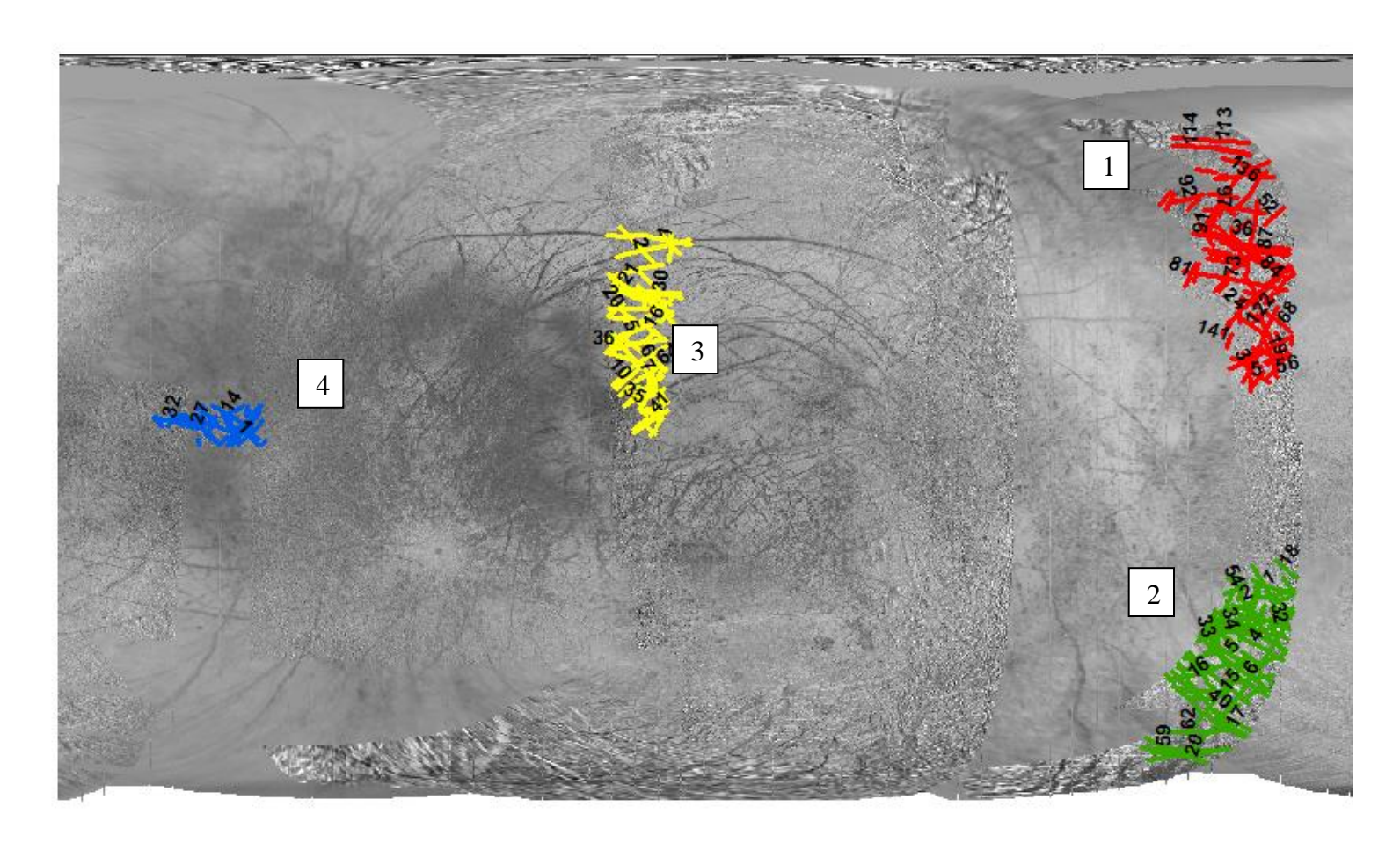


Fig. 4

The varying resolutions of different areas are shown here, with faults in areas of appropriate resolution shown in color. These areas are 1) North Leading Hemisphere, 2) Southern Leading Hemisphere, 3) North Trailing Hemisphere, and 4) West Equatorial Hemisphere

1:50,000,000 scale

I used a standard azimuth system measured from north and varying between 0 and 360 degrees for every mapped slip vector. The chosen self-consistent measurement method is to begin at the left-leading leg of the fault, and map along the strike to the rightmost leg. This is visually illustrated in figure 5, which also provides an example of a series of strike slip faults. From this, the polyline was entered into the data storage, so the azimuth, attitude, geodesic length, and coordinates could be extrapolated.

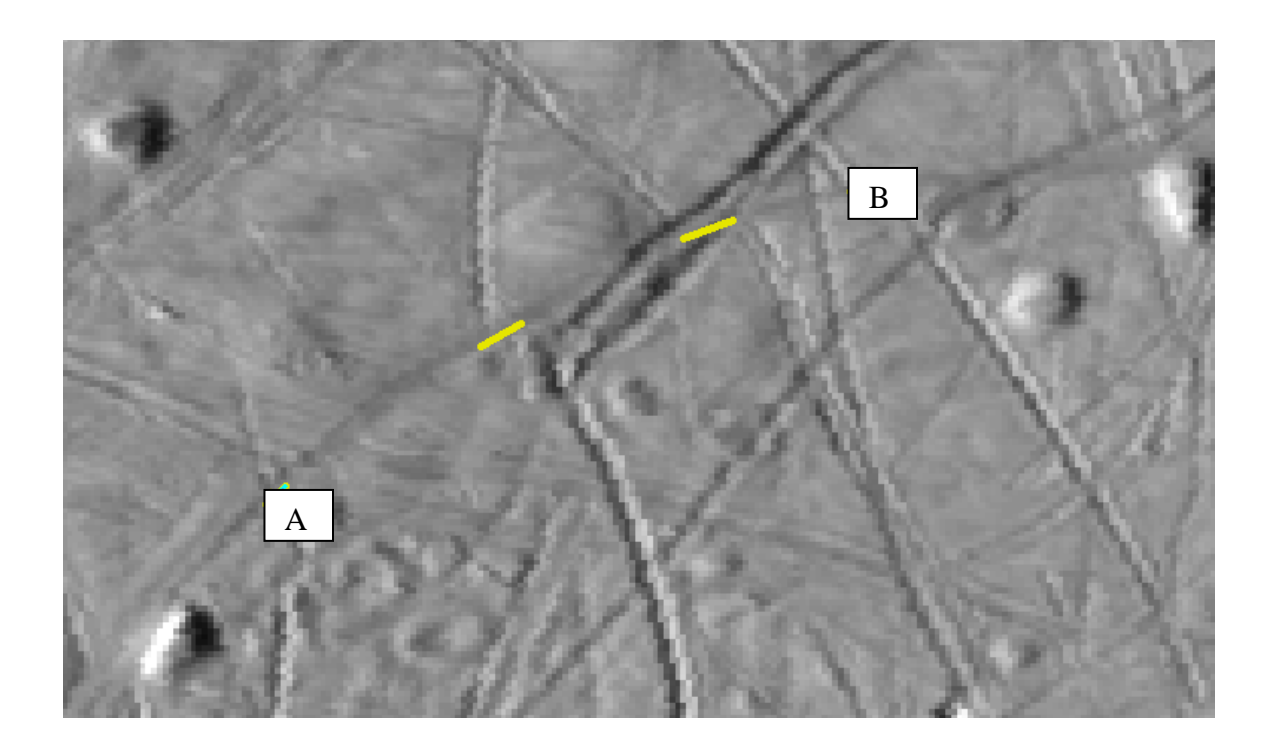


Figure 5

An example of a series of strike slip faults. The azimuth values range from 47 degrees (A) to 77 degrees (B). These all are left lateral faults, and that is determined both from visual observation as well as extrapolating from the azimuth values.

Once all of the major strike slip faults were mapped, the bearing, geodesic length, and coordinate location for each fault was compiled into categories based on regions, with the regions being used outlined in figure 4. From these three data sets, all other information could be calculated or inferred. For example, all azimuth values from 0° to 179° are left lateral faults, while all azimuth values from 180° to 359° are right lateral faults. A combination of Microsoft Excel and Matlab was used for the statistical analysis of these measured and inferred data values.

Presentation of Data:

ArcGIS as a program was designed for maps with arbitrary precision. Due to the spatial resolution of the Europan map and the objects being measured, the precision of measurements made by ArcGIS had to be limited. The initial, unaltered measurements of azimuth taken from the two point polylines averaged from 11 to 12 unrounded figures. This degree of precision would not be significant even without human error being taken into account. Each degree measurement was cut down to integers only as a method of error compensation for the azimuth. A similar issue arose with the geodesic length. Each length measurement contained seven to eight unnecessary significant figures. In addition to this, as shown in figure 6, each individual pixel available on the map was at least 500 m in both length and width. To represent this margin of error in the geodesic length measurements, all of the length values were rounded to the nearest 500 m.



Figure 6

A close up of the individual pixels, in order to measure an accurate spatial resolution. The pink line is exactly 500 m in length, and the pixels are square.

This pixel is located in the North Leading Hemisphere region.

A list including length and bearing of all 72 measured strike slip faults can be found in appendix I. Of the measured faults, 44 were categorized as right lateral, and 28 as left lateral. Figure 7 shows the azimuth plotted against the displacement, with symbology differing the right and left lateral points. The average azimuth for right lateral values is 261° while the average value for left lateral values is 89°. In addition to this information, for each strike slip polyline, a midpoint was collected (in latitude and longitude coordinates). A representation of collection areas on the surface of Europa is shown in figure 8, assembled by the coordinate values. Due to the spatial resolution and areas of the map used to find faults, the exact location is less useful

than the general information such as which hemisphere or quadrant of the map and how that affects the local strike slip faults. Figure 8 also displays the directions of slips in tandem with these locations. This figure shows that of the strike slip faults found and recorded in this project, the model made by Hoppa (2000) is not accurate. That attitude model predicted that the southern hemisphere would only be right lateral and the north would be left lateral, but the data found by this project nullifies that hypothesis.

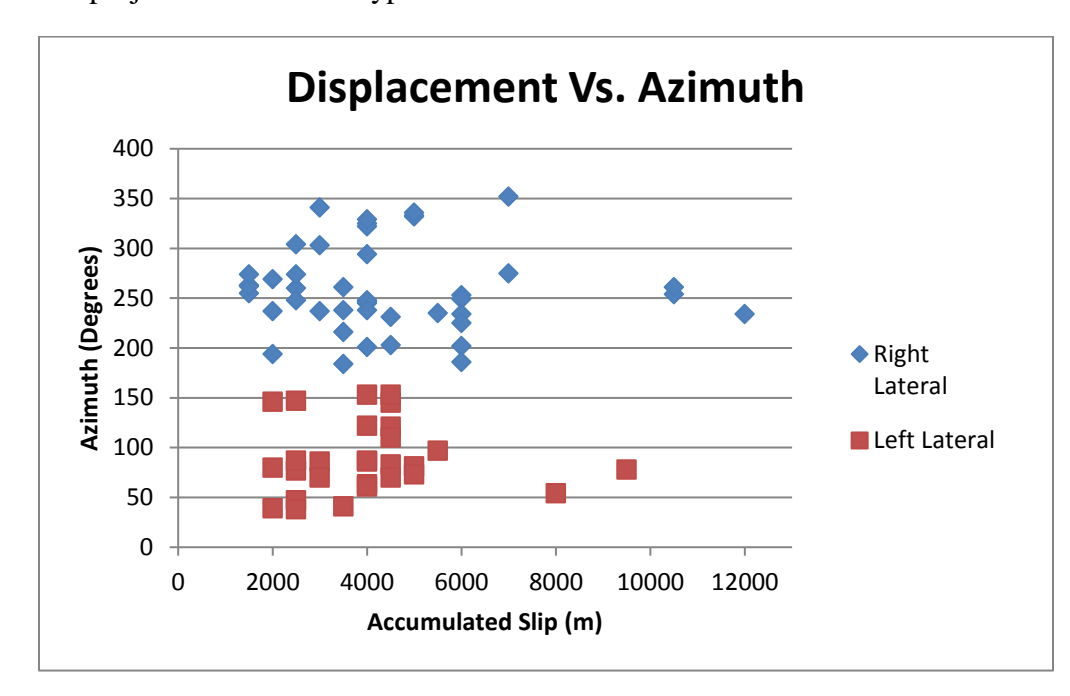
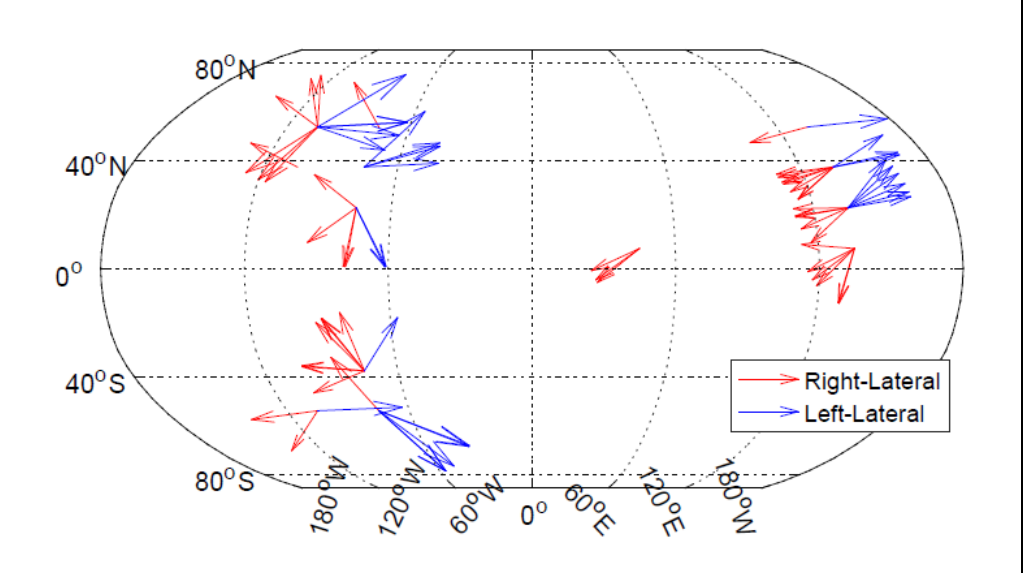


Fig. 7

Accumulated slip plotted against the azimuth of the 72 observed strike slip faults.



The location of the strike slip faults shown, in addition to their attitude and accumulated slip, shown by the length of the arrow.

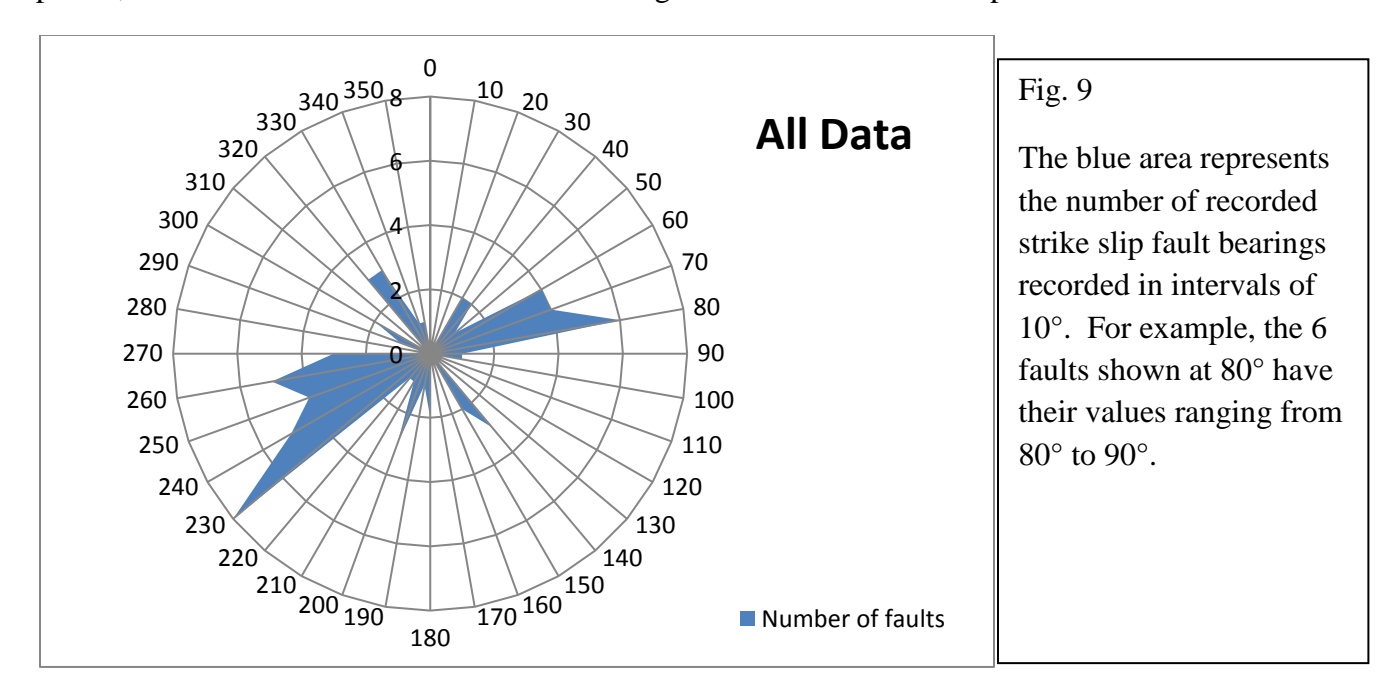
Fig. 8

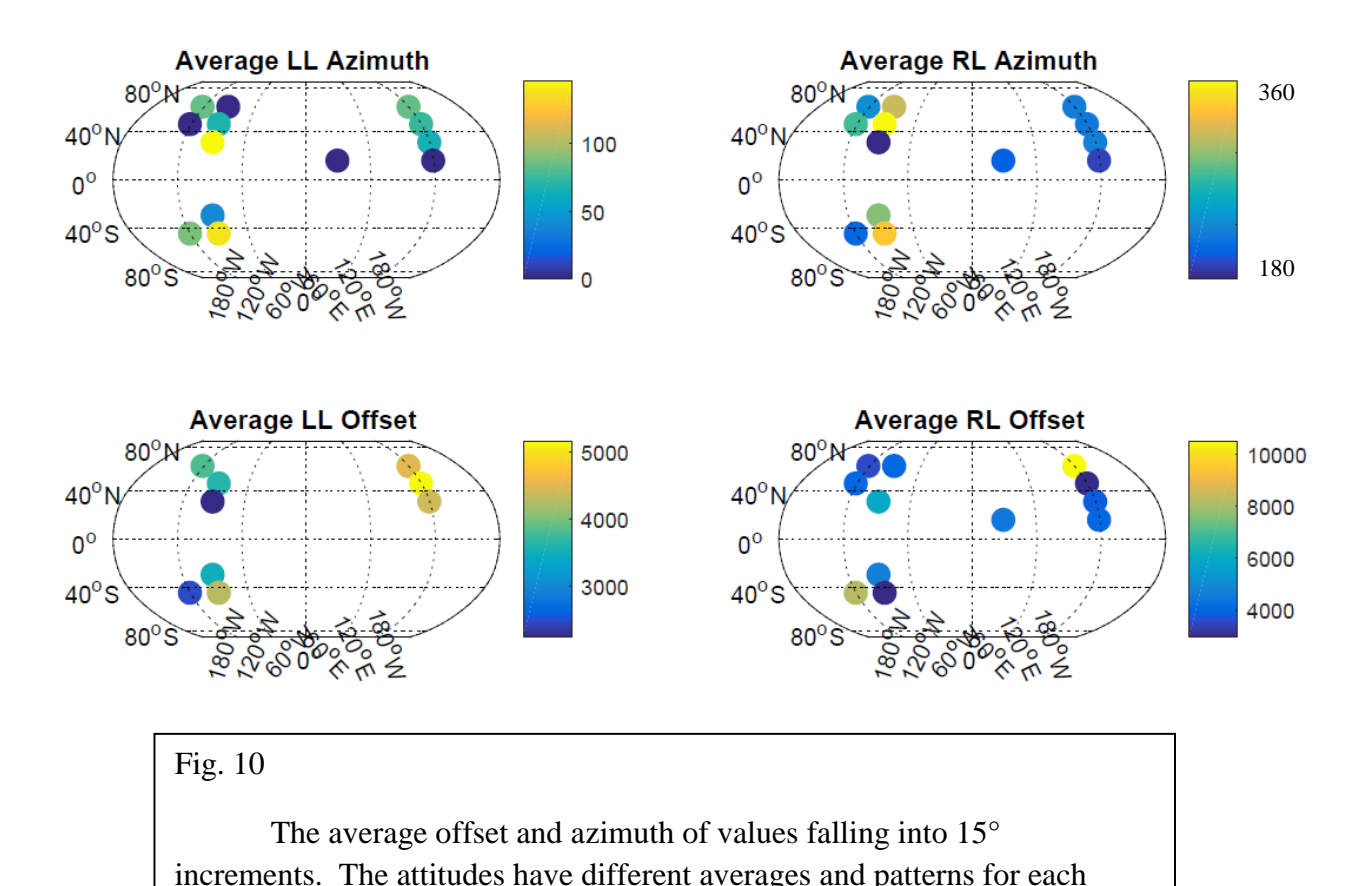
Discussion of Results:

The hypothesis being tested in this study is whether the azimuth of the observed slip vectors will show correlation with the accumulated slip of the strike slip faults on the surface of Europa. To test this hypothesis, only the azimuth and geodesic length are required from the collected data sets. When put into a graph directly comparing the two sets, such as figure 7, no clear pattern emerges. The introduction of a trend line also provides no clear pattern recognition. After converting the degrees into radians, a function was applied in Matlab which tests for circular correlation between a radian value and a linear value, which in this case is the azimuth (in degrees) and the accumulated slip distance (in meters). This function led to a correlation coefficient of 0.162 and a p value of 0.3888. A correlation coefficient this low is not statistically significant enough to justify a correlation. The p value, which would need a value below to 0.05 to statistically reject the null hypothesis, is greater than this by 0.3388, so the null fails to be rejected.

The averages of the right and left lateral strike slip faults are within 20° of being 180° apart. Looking at a diagram of all of the faults on a rose diagram, such as figure 9, shows that this average does represent the collected faults. Figure 10 shows the averages of each attitude at different coordinates throughout the moon. The four different regions each have a slight correlation in their values, both for average offset and average azimuth.

One variable which was unavailable to me using these analysis methods was time. We don't know the ages relative to each other for all of the strike slip faults. Superposition means we can infer that the lineament cross cutting the of the strike slip faults is oldest. To effectively test for the time variable, we must obtain the correlation of bearing and offset during a certain time period, which uses data that is not available using the resolution of this map.



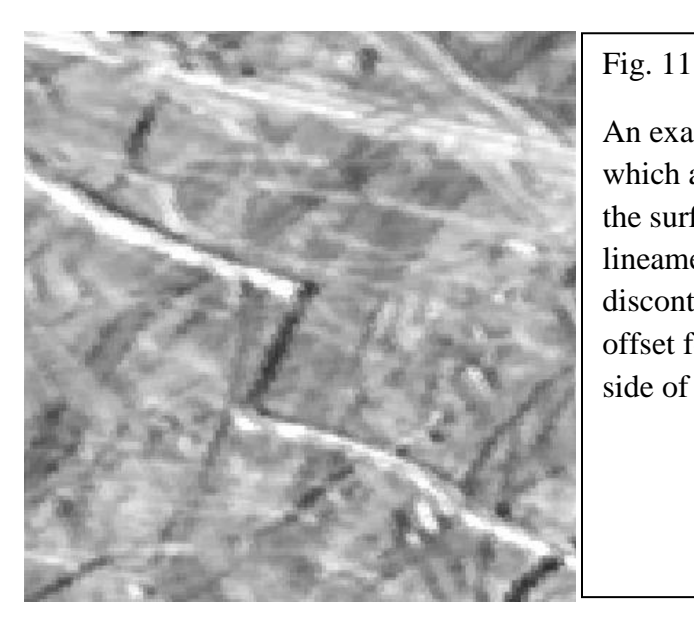


Suggestions for Future Work:

region as well.

Further work on this moon would be necessary to understand some of the mechanics found during this project. The primary hindrance of further investigation would be the spatial resolution of the available map. The temporal, radiometric, and spectral resolution are also all lacking, since there is only one map available in a narrow wavelength band, but it is the spatial resolution of this mosaic map which limited this project the most. It is almost definite that there are more than 72 strike slip faults on the surface of this moon, but actually seeing and measuring all of them in any detail would be impossible with the current map available. Entire regions have only been imaged at spatial resolutions of multiple kilometer magnitudes per pixel. With higher resolution images, a much more in depth analysis could be carried out on the surface of Europa. Acquiring such a map, however, would require a higher resolution and perhaps closer flyby by a Jovian probe.

Another potential area of research which is relatively unexplored are the unusual features termed "Jogs" for the purpose of this explanation. These counterintuitive surface lineaments, while not going unnoticed, are still unexplained. An example of one is shown in figure 11 where the jog otherwise would be an example of a strike slip fault, if not for the lack of any continuity features to either side. The lineament proceeds to a juncture, an unknown force (assumedly) changes the propagation direction, and there is a near 90° turn made. The lineament propagates in that direction for some distance and then makes another 90° turn to resume its previous direction.



An example of the "Jogs" which are prevalent on the surface of Europa as lineaments. Note the discontinuity of any offset features to either side of the lineament.

In the process of looking for true strike slip faults, 24 of these jogs were found, with varying lengths which tended to be, on average, higher than that of the strike slip faults by about a factor of 10. The range of azimuths of these jogs was much higher than the individual right or left lateral strike slip faults, but the average was 171°. Intriguingly, that is almost exactly 90° from both right (261°) and left (89°) lateral faults. When the displacement and bearing of slip were run through the same statistical test, the correlation coefficient came out as 0.2414, which is greater than that of the original data set that was the subject of this research. The p value, however, is even higher, being 0.497, so the correlation is likely to have occurred by chance. A full accounting of all these jogs can be found in appendix VI as well as graphically represented in figure 12.

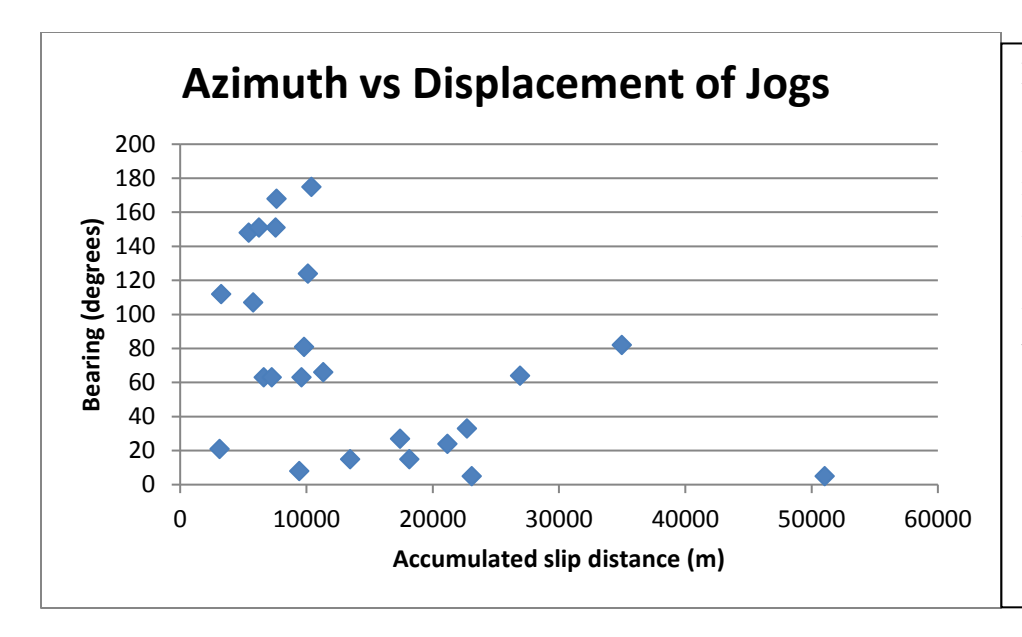


Fig. 12

A greater range of values is shown here among the Displacement vs. azimuth of the jogs, with the meters slipped larger by magnitudes of ten.

Conclusions:

In this study, we mapped the azimuth and offset on strike slip faults on Europa, in order to test the hypothesis that the offset correlates with azimuth. However, due to insignificant significance of the correlation between the geodesic length of the displacement and the bearing of the fault, the null hypothesis fails to be rejected. This means that there is no statistically significant correlation between these two aspects of the faults, at the least among those faults observed. In other terms, this evidence would suggest that there is not a consistent force pulling steadily in one direction on the icy surface of Europa, or that there was another factor, such as time, which was interfering with the strike slip faults enough to nullify any correlation. A rejected null hypothesis would have meant that there was a steady and noticeable strain vector acting on the crust, caused by one of a variety of forces. The fact that the rejection of the null failed means that if such a strain vector exists, it cannot be described by an aspect of the strike slip faults or by the two descriptor data categories used. One other relationship that was described by Hoppa (2000) was that there are more left lateral strike slip faults on the northern hemisphere, and these surface lineaments and some faults are formed by the libration of the moon. My findings verify this because, if there was a 50% chance of a fault being left or right lateral, then using a binomial probability, there is only a 1.59% chance that the results I found would have been acquired. This is consistent with the statistical significance of the disparity between the number of faults of each attitude. However, going against Hoppa's findings, the data I collected has a much higher number of right lateral faults than left lateral, while a full 25% of the recorded left lateral faults were in the southern hemisphere, compared to 22% of the right lateral faults.

Bibliography:

Carr, M. H., Belton, M. J., Chapman, C. R., Davies, M. E., Geissler, P., Greenberg, R., McEwen, A. S., Tufts, B. R., Greeley, R., Sullivan, R., Head, J. W., Pappalardo, R. T., Klaasen, K. P., Johnson, T. V., Kaufman, J., Senske, D., Moore, J., Neukum, G., Schubert, G., Burns, J. A., Thomas, P., & Veverka, J. (1998). Evidence for a subsurface ocean on Europa. *Nature*, 391(6665), 363-365.

Culha, C., Hayes, A. G., Manga, M., & Thomas, A. M. "Double ridges on Europa accommodate some of the missing surface contraction." *Journal of Geophysical Research: Planets* 119.3 (2014): 395-403.

Goldreich, P. M., & Mitchell, J. L. (2010). Elastic ice shells of synchronous moons: Implications for cracks on Europa and non-synchronous rotation of Titan. *Icarus*, 209(2), 631-638. doi:10.1016/j.icarus.2010.04.013

Hoppa, G., Greenberg, R., B. Tufts, P. Geissler, C. Phillips, & M. Milazzo. "Distribution of strike-slip faults on Europa." *Journal of Geophysical Research: Planets* 105.E9 (2000): 22617-22627.

Ip, W.-H., Kopp, A., Williams, D. J., McEntire, R. W., & Mauk, B. H. (2000). Magnetospheric ion sputtering: The case of Europa and its surface age. *Advances In Space Research*, 26(10), 1649-1652. doi:10.1016/S0273-1177(00)00112-5

Jin, S., & Ji, J. (2012). The internal structure models of Europa. *Science China Physics, Mechanics And Astronomy*, 55(1), 156-161. doi:10.1007/s11433-011-4573-9

Rhoden, A., Wurman, G., Huff, E., Manga, M., & Hurford, T. "Shell tectonics: A mechanical model for strike-slip displacement on Europa." *Icarus* 218.1 (2012): 297-307.

Rhoden, A. R., Hurford, T. A., Roth, L., & Retherford, K. (2015). Linking Europa's plume activity to tides, tectonics, and liquid water. *Icarus*, *253*, 169-178. doi:10.1016/j.icarus.2015.02.023

Rhoden, A. R., & Hurford, T. A. "Lineament azimuths on Europa: Implications for obliquity and non-synchronous rotation." *Icarus* 226.1 (2013): 841-859.

Sarid, A. R., Greenberg, R., & Hurford, T. A. "Crack azimuths on Europa: Sequencing of the northern leading hemisphere." *Journal of Geophysical Research: Planets* 111.E8 (2006).

Schenk, P. M., McKinnon, W. B. "Fault offsets and lateral crustal movement on Europa." *Reports of Planetary Geology and Geophysics Program* (1985).

Appendix I

Bearing, length, and attitude of all 72 strike slip faults

ld	Length	Bearing	Attitude
			LL
1	4500	83	
2	10500	254	RL
3	2500	260	RL
4	2000	80	LL
5	1500	255	RL
6	4000	245	RL
7	2000	237	RL
8	4000	63	LL
9	9500	78	LL
10	3000	237	RL
11	1500	263	RL
12	6000	253	RL
13	6000	249	RL
14	1500	262	RL
15	2000	269	RL
16	3500	261	RL
17	2500	77	LL
18	4500	70	LL
19	4000	61	LL
20	2500	47	LL
21	8000	54	LL
22	5000	81	LL
23	6000	234	RL
24	4500	231	RL
25	4500	203	RL
26	1500	274	RL
27	6000	202	RL
28	4000	247	RL
29	3500	238	RL
30	4000	325	RL
31	7000	275	RL
32	2500	274	RL
33	2500	248	RL
34	5000	333	RL
35	5000	332	RL
36	7000	352	RL
37	3500	41	LL
38	4000	153	LL
39	4500	145	LL
40	4500	121	LL
41	3000	341	RL
42	6000	225	RL
43	4000	122	LL
44	4500	153	LL
45	10500	261	RL
46	2500	87	LL
47	3000	303	RL
<u> </u>	3000		·

Length in meters

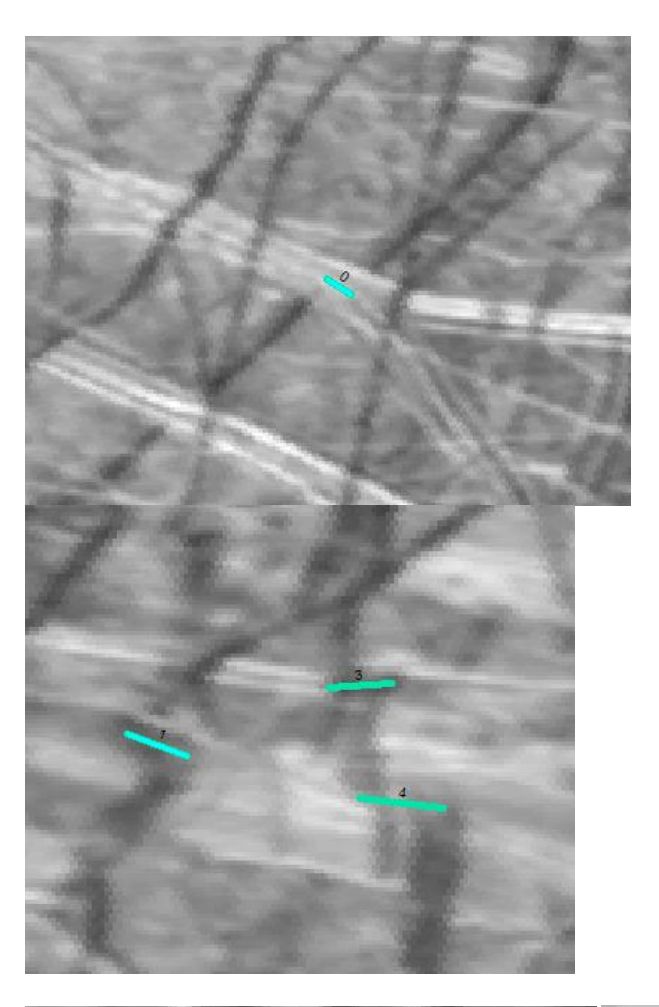
Bearing in degrees clockwise from north

Attitude symbols represent Left
Lateral (LL) and Right Lateral (RL)

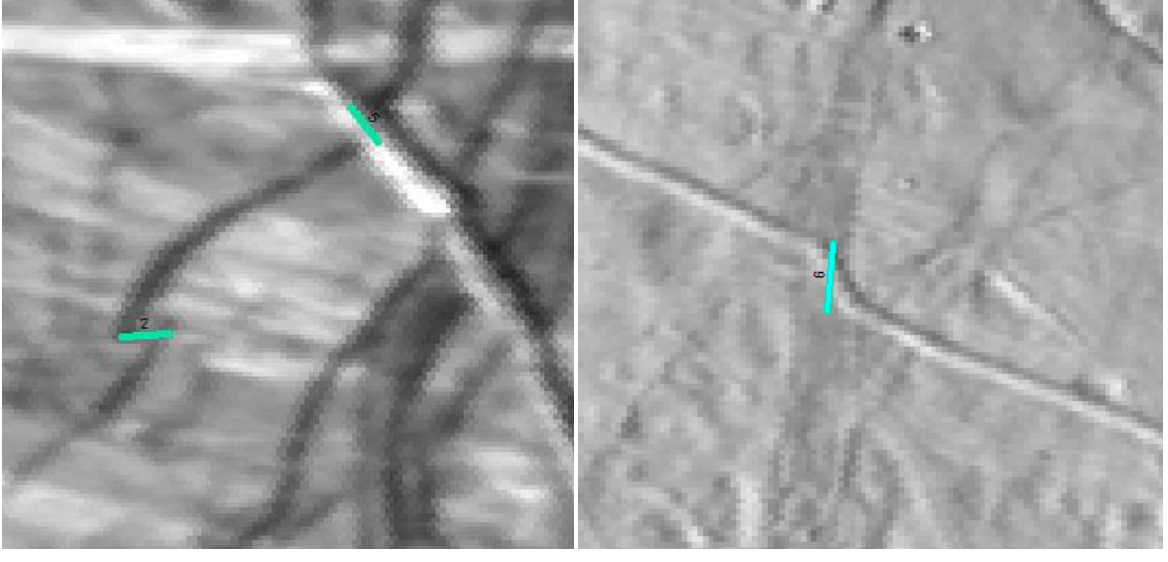
48	4500	110	LL
49	3000	86	LL
50	4000	86	LL
51	5500	97	LL
52	4000	322	RL
53	6000	186	RL
54	12000	234	RL
55	4000	294	RL
56	3000	70	LL
57	5000	73	LL
58	4000	87	LL
59	2500	38	LL
60	2500	147	LL
61	2000	146	LL
62	3500	184	RL
63	2500	304	RL
64	3500	216	RL
65	2000	194	RL
66	4000	329	RL
67	2000	39	LL
68	5000	336	RL
69	4000	201	RL
70	4000	248	RL
71	4000	238	RL
72	5500	235	RL

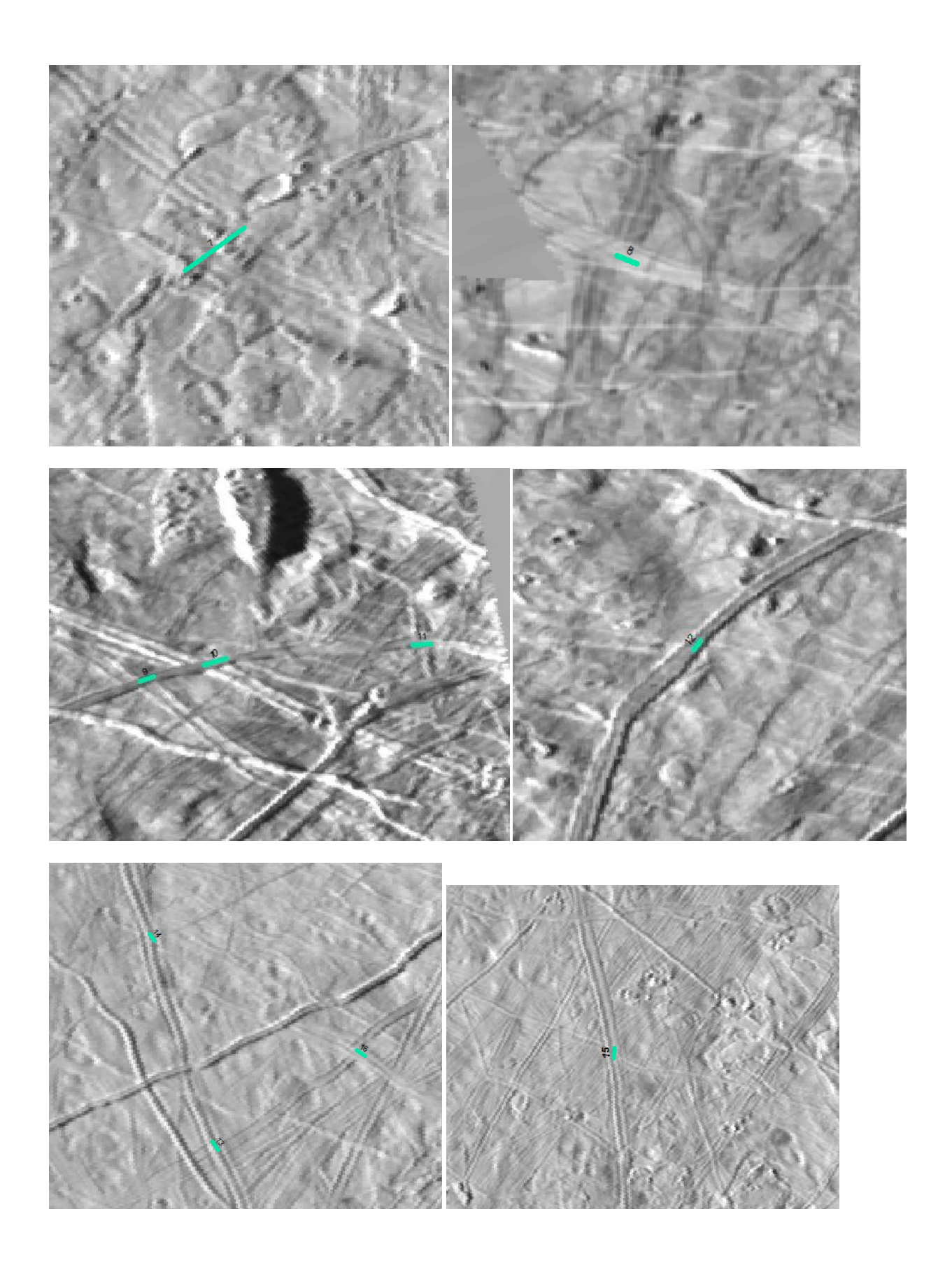
Appendix II

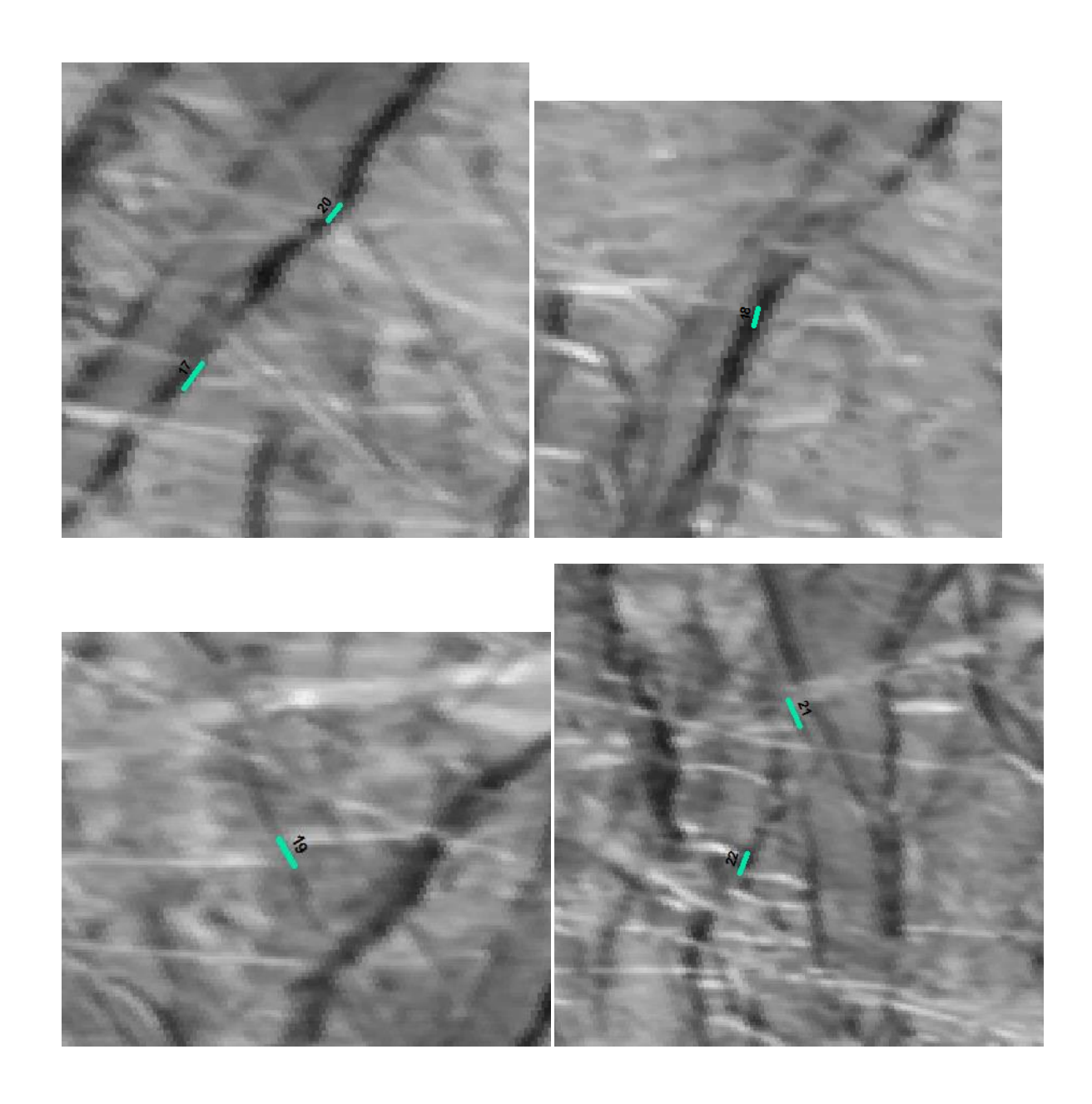
All strike slip faults in the north leading region



FID	Length	Bearing
0	3000	303
1	4500	110
2	3000	86
3	4000	86
4	5500	97
5	4000	322
6	6000	186
7	12000	234
8	4000	294
9	3000	70
10	5000	73
11	4000	87
12	2500	38
13	2500	147
14	2000	146
15	3500	184
16	2500	304
17	3500	216
18	2000	194
19	4000	329
20	2000	39
21	5000	336
22	4000	201

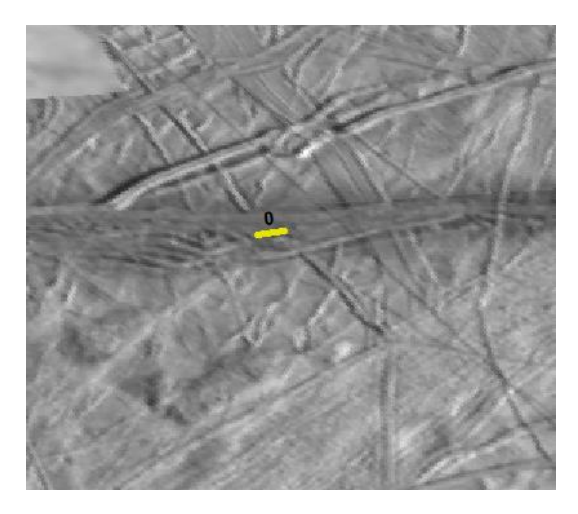


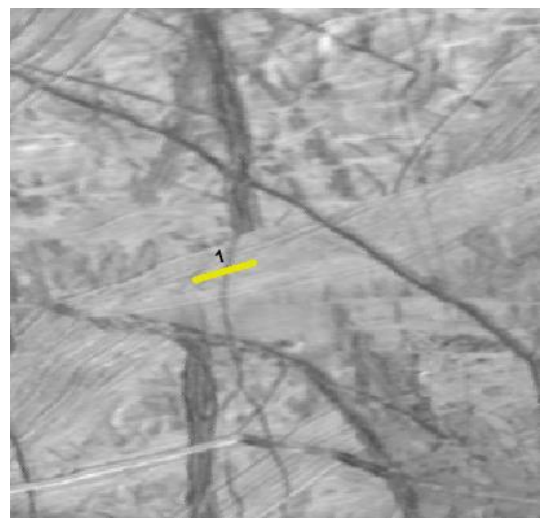




Appendix III

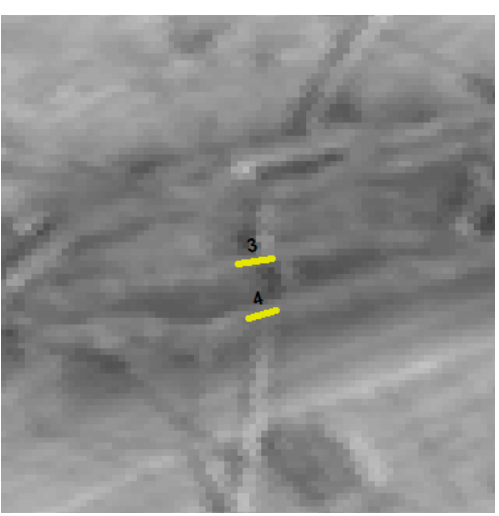
All strike slip faults in the north trailing region

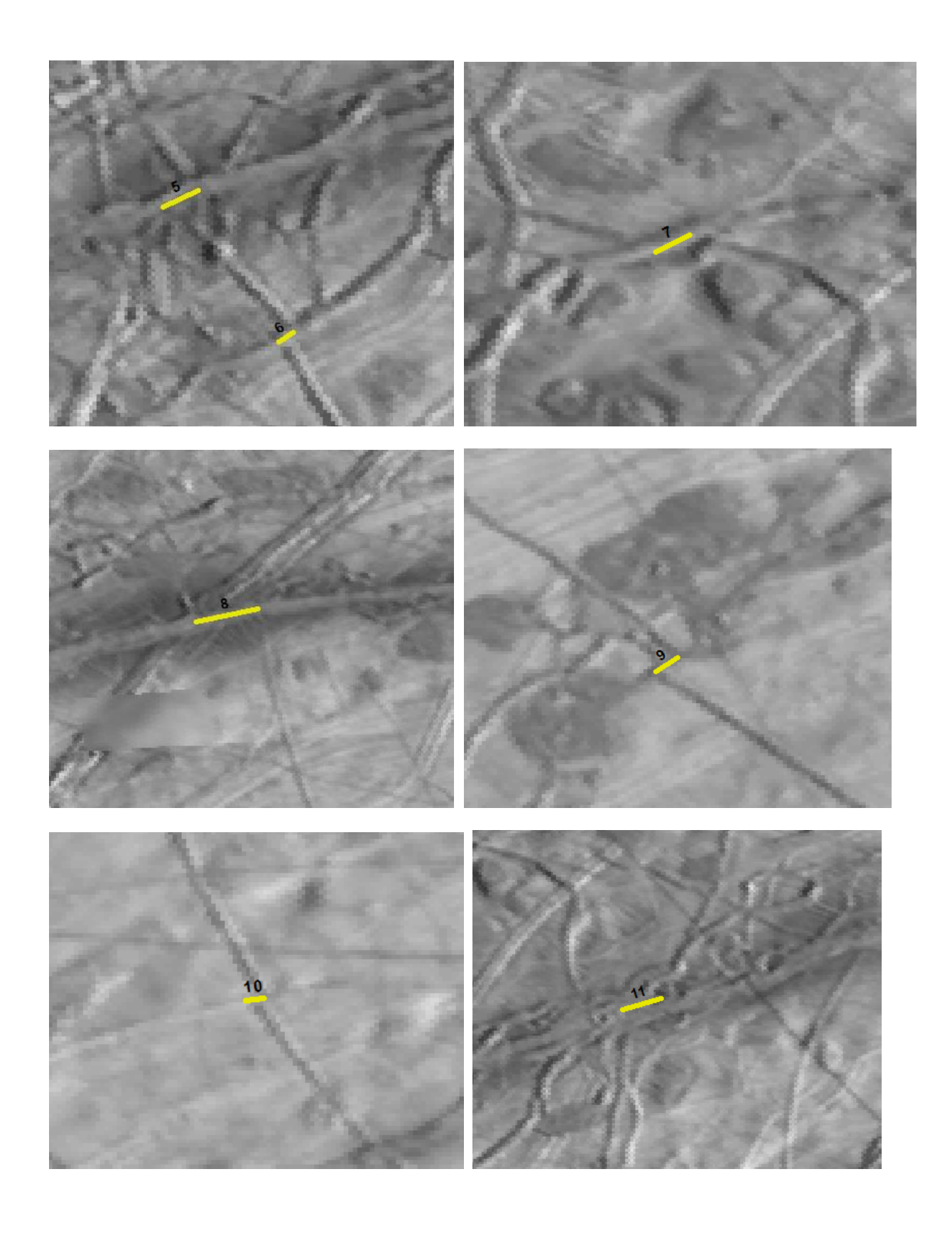


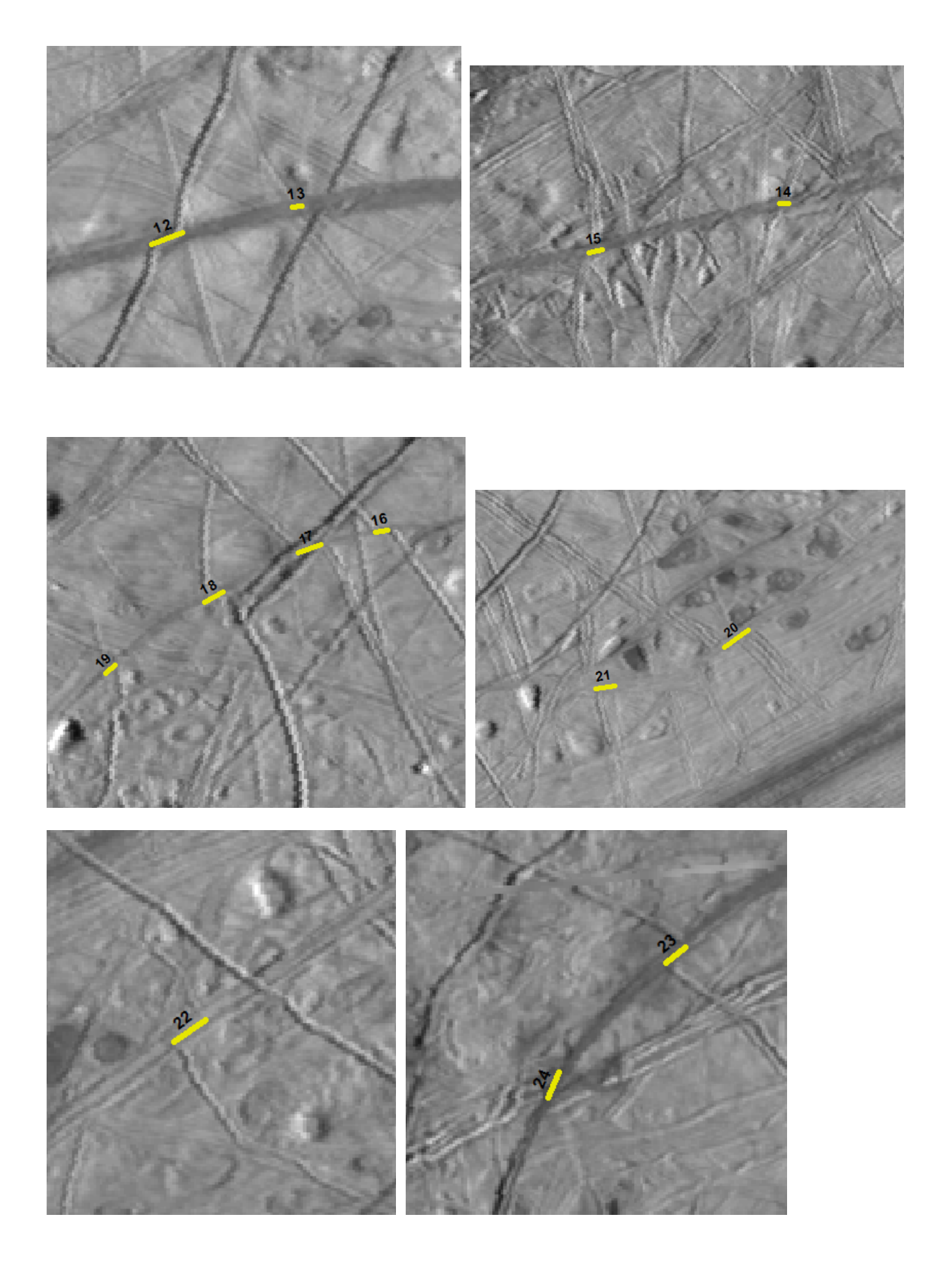


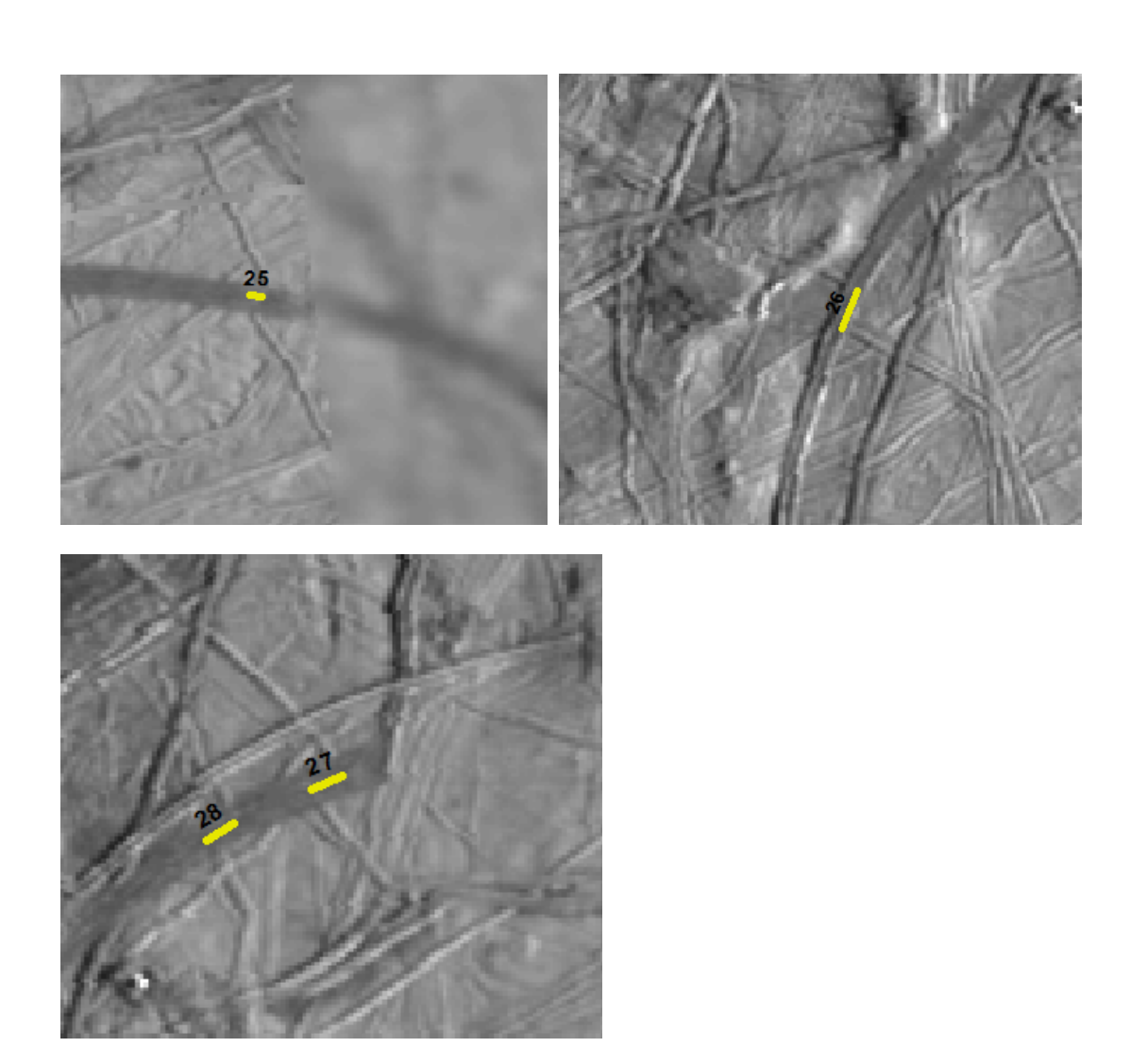
FID	Length	Bearing
0	4500	83
1	10500	254
2	2500	260
3	2000	80
4	1500	255
5	4000	245
6	2000	237
7	4000	63
8	9500	78
9	3000	237
10	1500	263
11	6000	253
12	6000	249
13	1500	262
14	2000	269
15	3500	261
16	2500	77
17	4500	70
18	4000	61
19	2500	47
20	8000	54
21	5000	81
22	6000	234
23	4500	231
24	4500	203
25	1500	274
26	6000	202
27	4000	247
28	3500	238





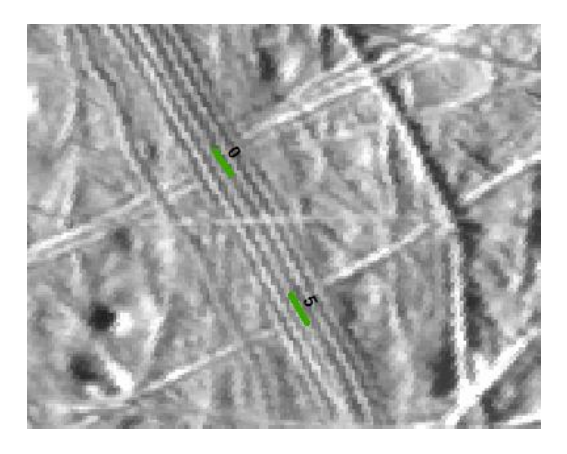


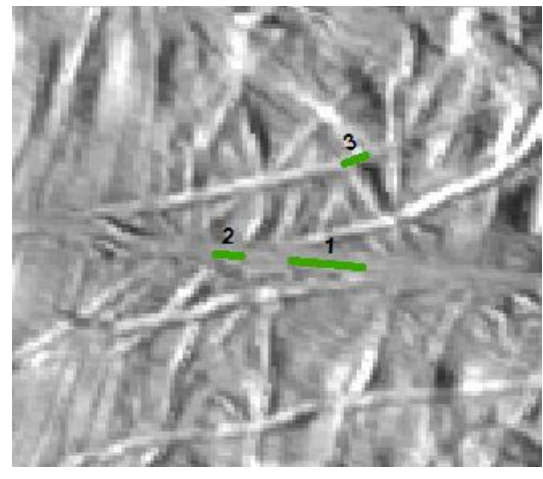




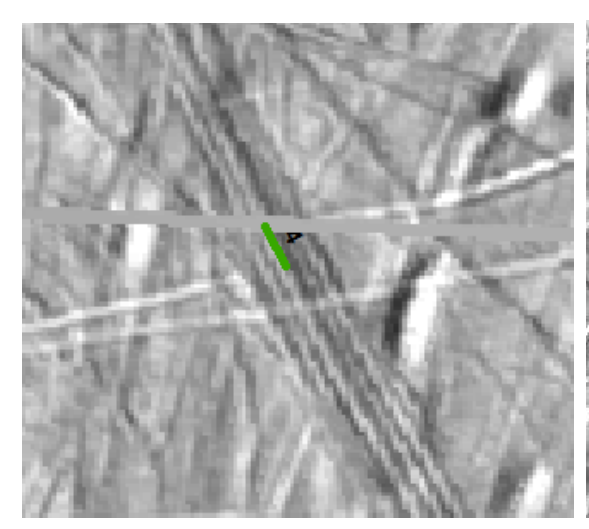
Appendix IV

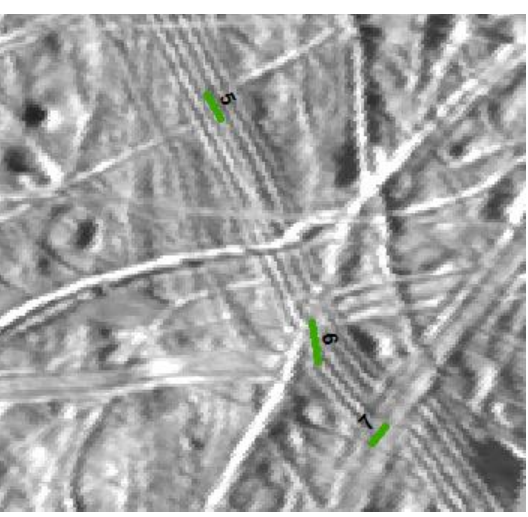
All strike slip faults in the south leading region

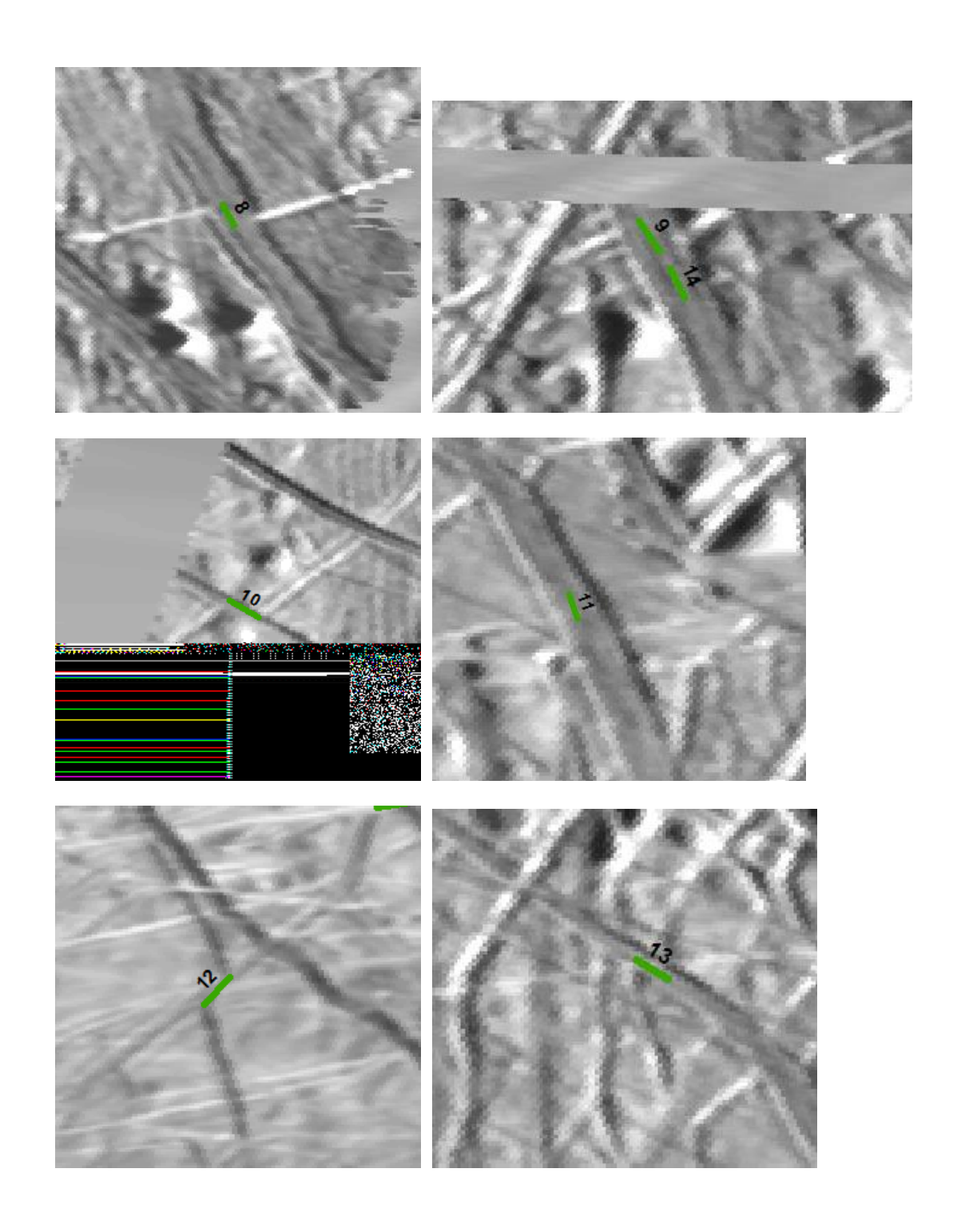


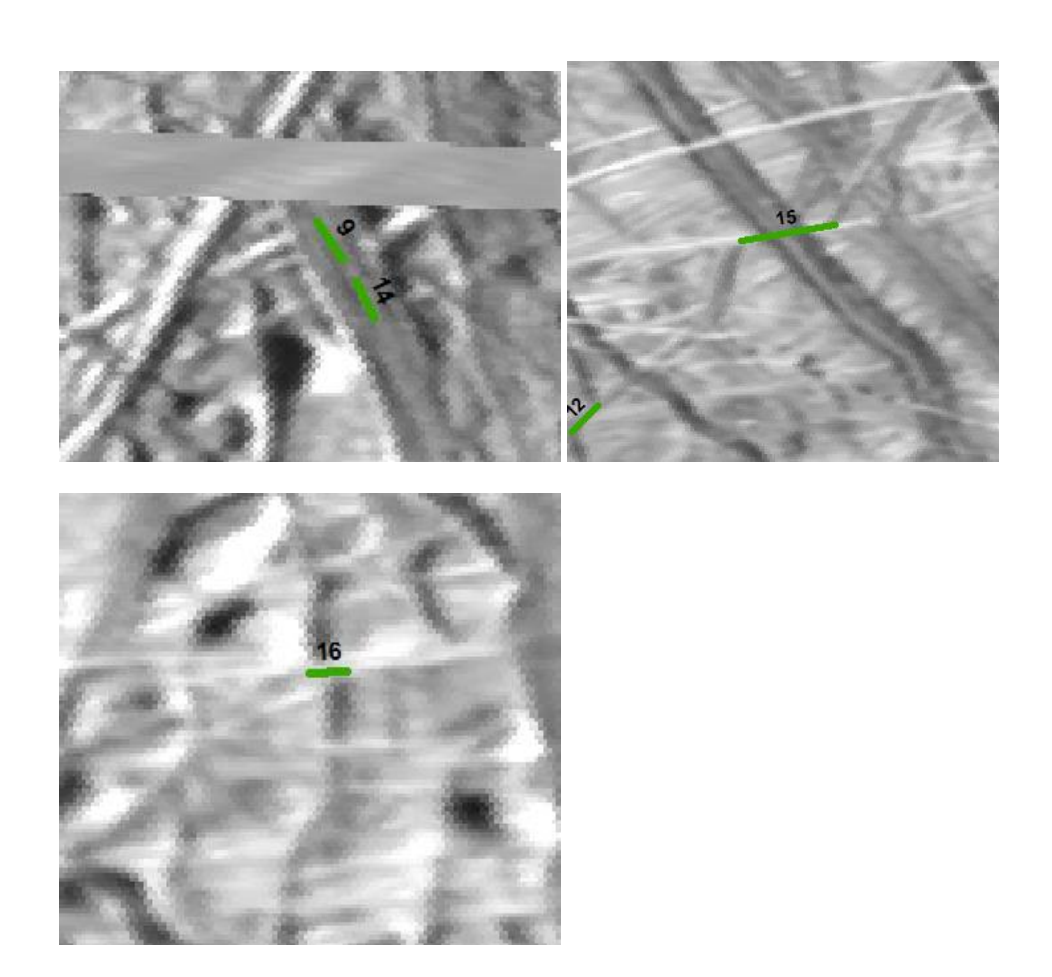


FID	Length	Bearing
0	4000	325
1	7000	275
2	2500	274
3	2500	248
4	5000	333
5	5000	332
6	7000	352
7	3500	41
8	4000	153
9	4500	145
10	4500	121
11	3000	341
12	6000	225
13	4000	122
14	4500	153
15	10500	261
16	2500	87



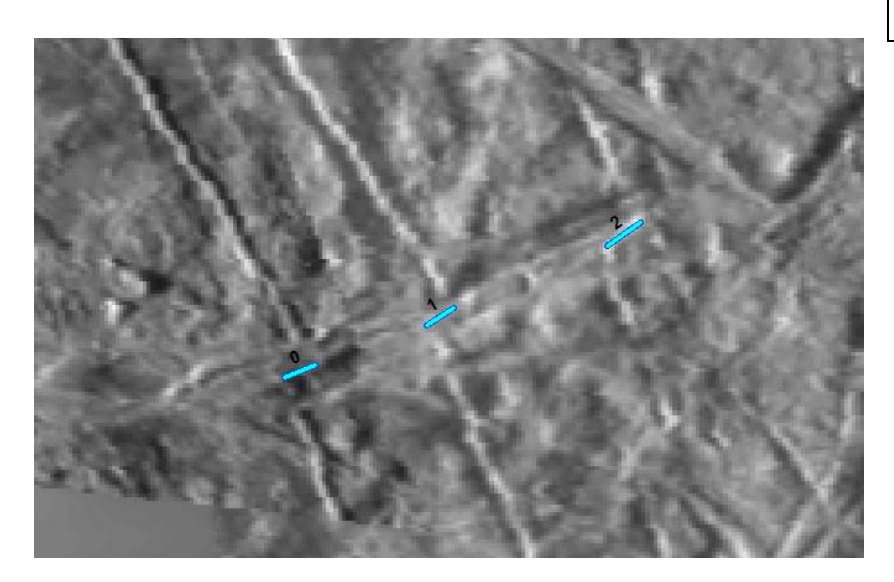






Appendix V

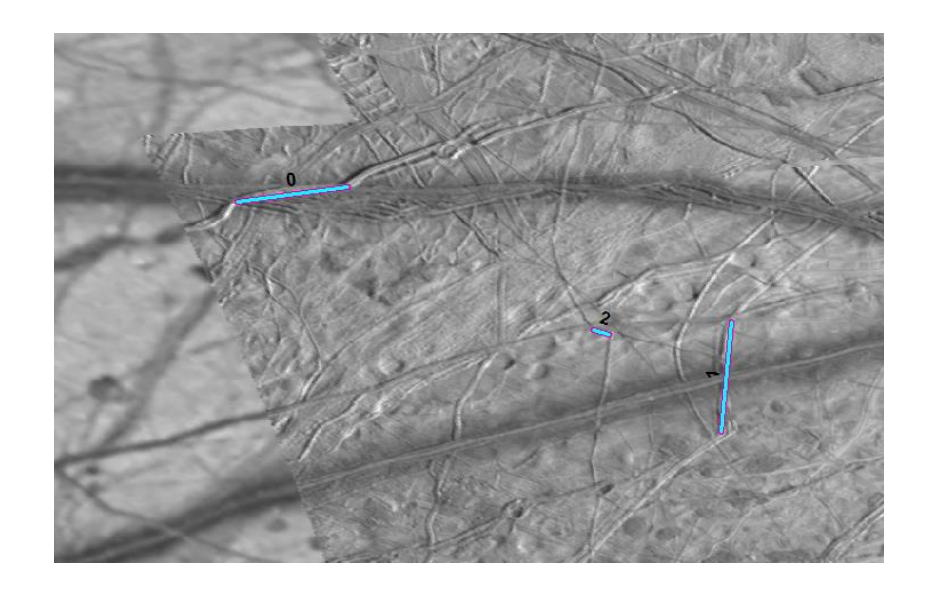
All strike slip faults of the western equatorial region

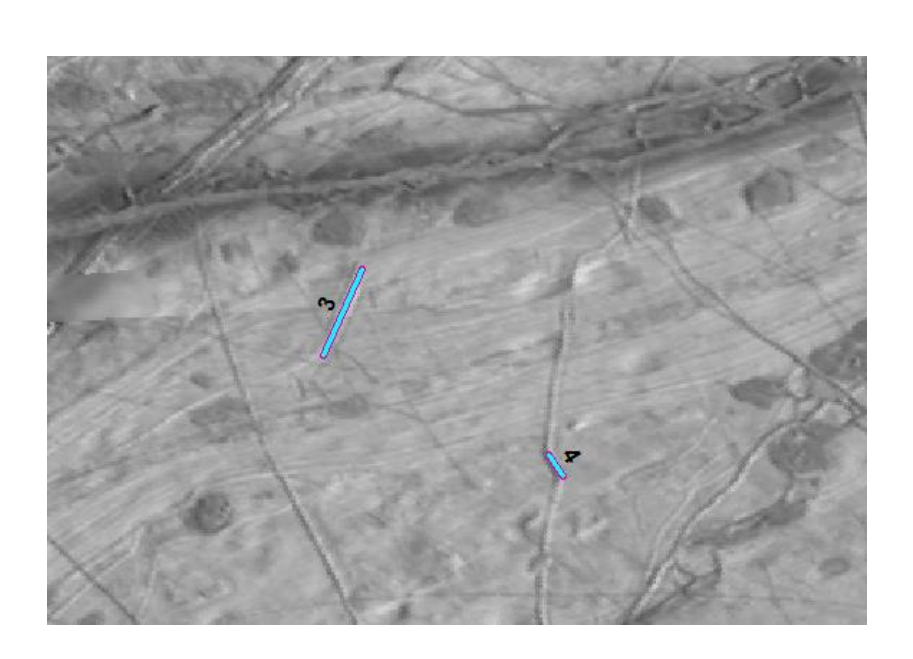


FID	Length	Bearing
0	4000	248
1	4000	238
2	5500	235

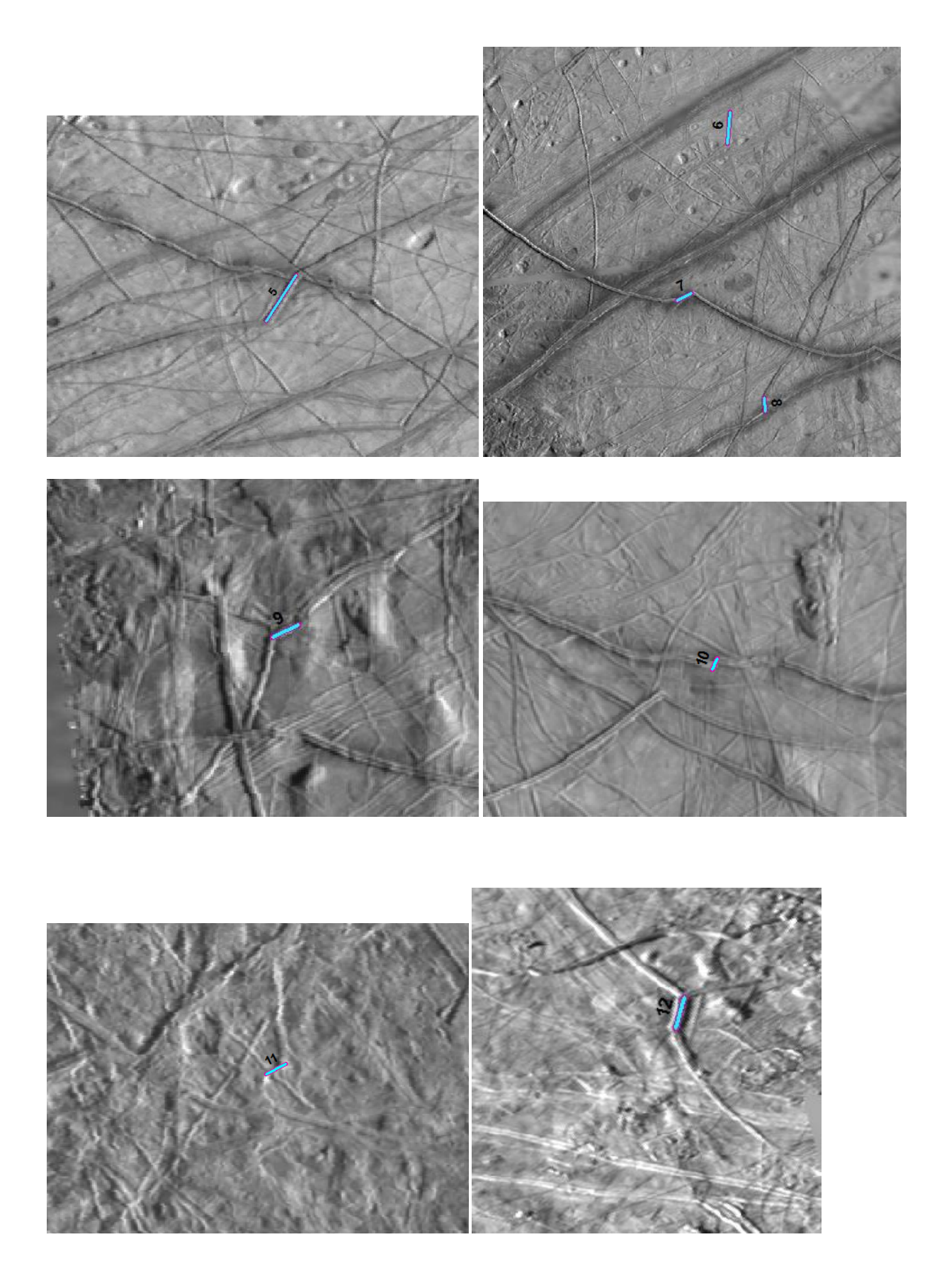
Appendix VI

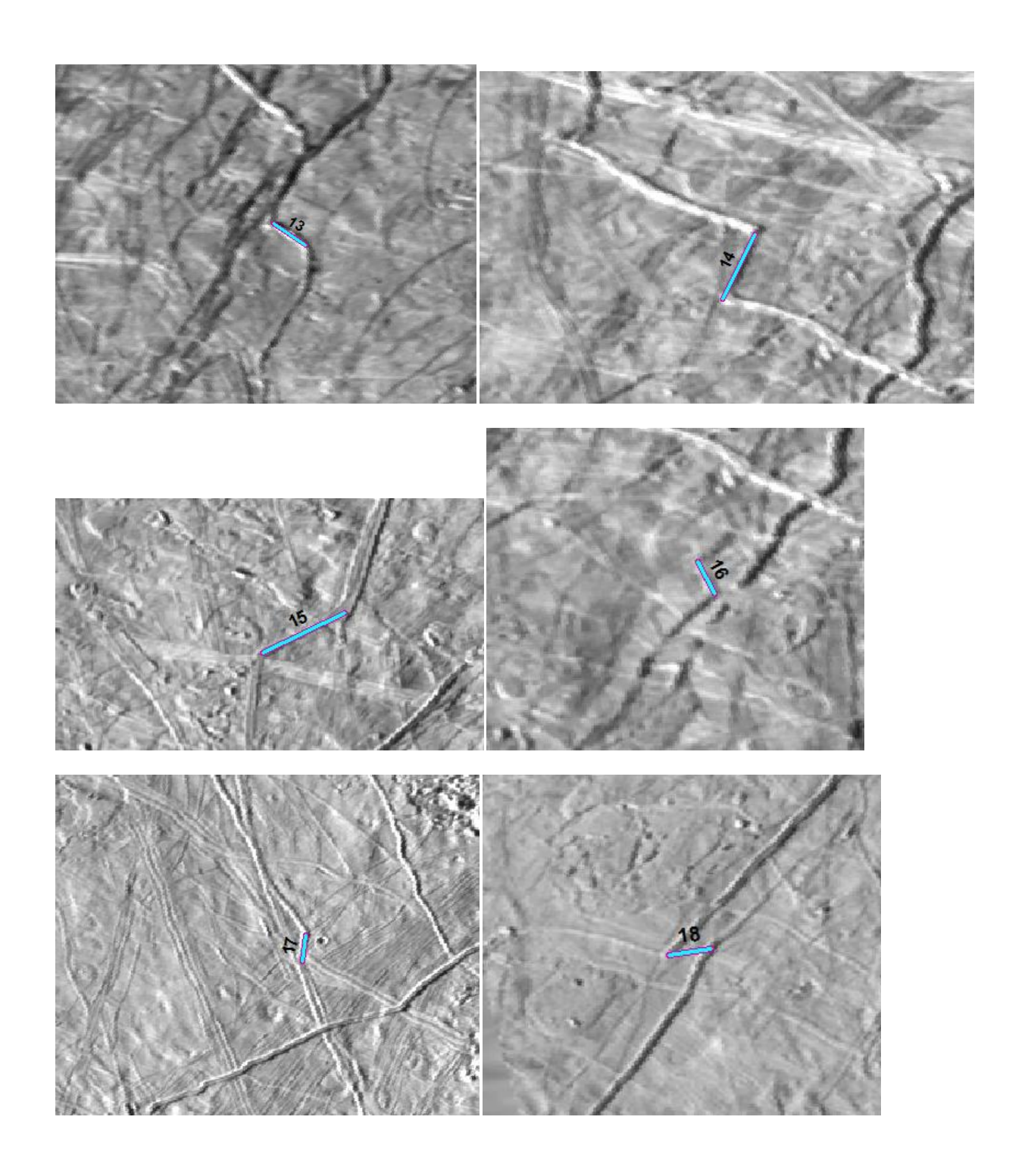
All jogs

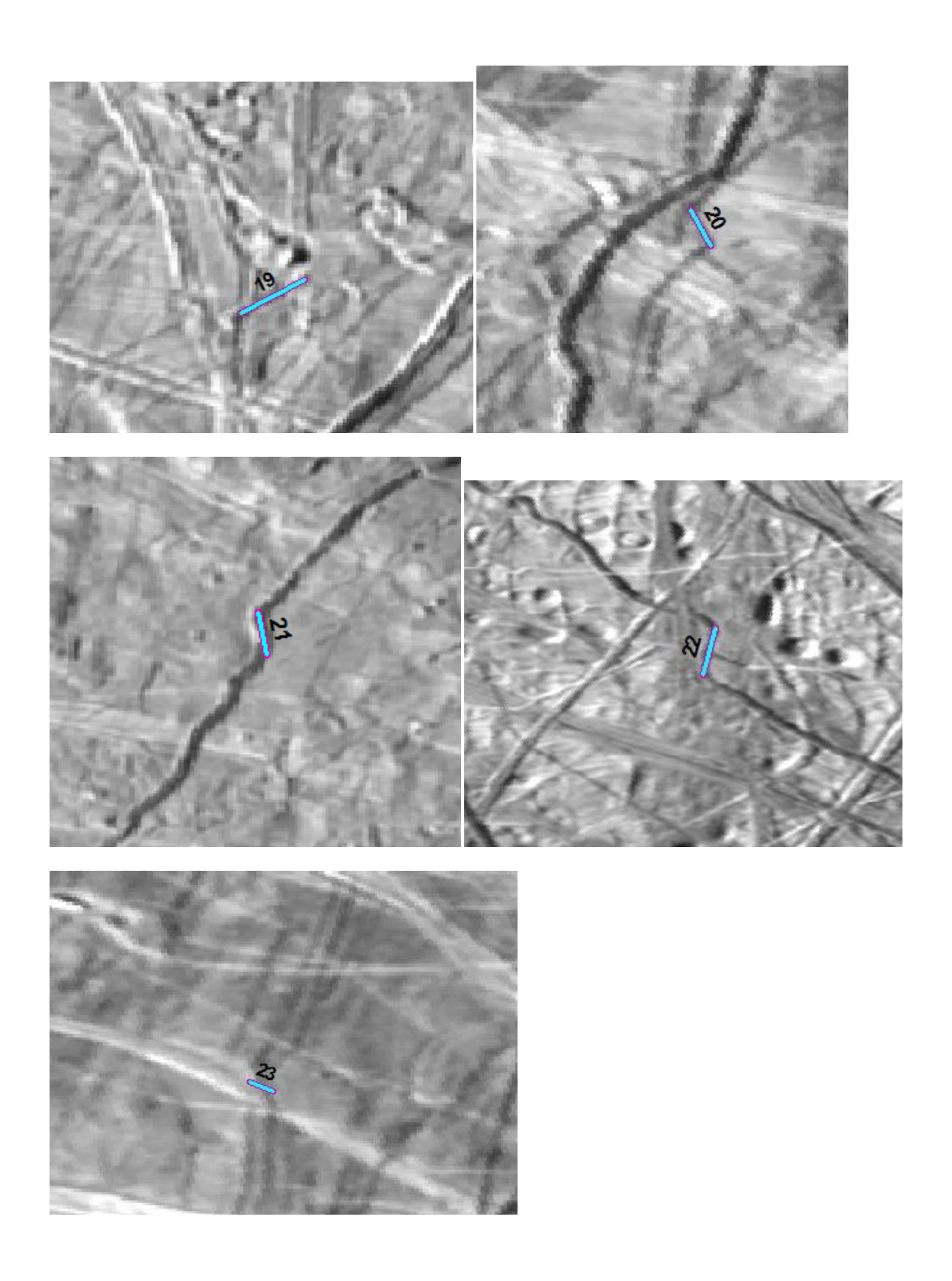




FID	Length	Bearing
0	35000	82
1	51000	5
2	6000	287
3	21000	24
4	5500	328
5	22500	33
6	23000	5
7	11500	66
8	10500	355
9	6500	243
10	3000	21
11	7500	243
12	13500	195
13	10000	124
14	17500	27
15	27000	244
16	7500	331
17	9500	188
18	10000	81
19	9500	243
20	6000	331
21	7500	348
22	18000	195
23	3500	112







Honor Code

I pledge on my honor that I have not given or received any unauthorized assistance on this assignment.